Requirement of Histidine 217 for Ubiquinone Reductase Activity (Q_i Site) in the Cytochrome bc_1 Complex†

Kevin A. Gray,*,‡ P. Leslie Dutton,§ and Fevzi Daldal‡

Department of Biology, Plant Science Institute, and Department of Biochemistry and Biophysics, Johnson Research Foundation, The University of Pennsylvania, Philadelphia, Pennsylvania 19104

Received June 24, 1993; Revised Manuscript Received October 18, 1993®

ABSTRACT: Folding models suggest that the highly conserved histidine 217 of the cytochrome *b* subunit from the cytochrome bc_1 complex is close to the quinone reductase (Q_i) site. This histidine (*b*H217) in the cytochrome *b* polypeptide of the photosynthetic bacterium *Rhodobacter capsulatus* has been replaced with three other residues, aspartate (D), arginine (R), and leucine (L). *b*H217D and *b*H217R are able to grow photoheterotrophically and contain active cytochrome bc_1 complexes (60% of wild-type activity), whereas the *b*H217L mutant is photosynthetically incompetent and contains a cytochrome bc_1 complex that has only 10% of the wild-type activity. Single-turnover flash-activated electron transfer experiments show that cytochrome b_H is reduced via the Q_o site with near native rates in the mutant strains but that electron transfer between cytochrome b_H and quinone bound at the Q_i site is greatly slowed. These results are consistent with redox midpoint potential (E_m) measurements of the cytochrome *b* subunit hemes and the Q_i site quinone. The E_m values of cyt b_L and b_H are approximately the same in the mutants and wild type, although the mutant strains have a larger relative concentration of what may be the high-potential form of cytochrome b_H, called cytochrome b_{150}. However, the redox properties of the semiquinone at the Q_i site are altered significantly. The Q_i site semiquinone stability constant of *b*H217R is 10 times higher than in the wild type, while in the other two strains (*b*H217D and *b*H217L) the stability constant is much lower than in the wild type. Thus H217 appears to have major effects on the redox properties of the quinone bound at the Q_i site. These data are incorporated into a suggestion that H217 forms part of the binding pocket of the Q_i site in a manner reminiscent of the interaction between quinone bound at the Q_b site and H190 of the L subunit of the bacterial photosynthetic reaction center.

Ubihydroquinone–cytochrome *c* oxidoreductase (the cytochrome bc_1 complex)[1] is an integral membrane protein involved in energy transduction in a wide range of organisms [for recent reviews see Trumpower (1990) and Cramer and Knaff (1990)]. The enzyme is a component of the mitochondrial electron transfer chain and performs a similar function in aerobic prokaryotes. Cytoplasmic membranes of anoxygenic photosynthetic prokaryotes also contain a cyt bc_1 complex which is utilized for both light-driven electron transfer and dark respiration (Dutton, 1986; Prince, 1990; Knaff, 1993). Chloroplasts of oxygenic organisms contain a similar redox complex (called the cyt b_6f complex) which functions between photosystems I and II. In all cases the complexes oxidize and reduce the lipid-soluble two-electron carrier (plasto-, ubi- or menahydroquinone) in the membrane phase and reduce a water-soluble one-electron carrier (cyt *c* or plastocyanin) at the membrane aqueous interface. During electron transfer, charges (as electrons and protons) are vectorially transported across the membrane, thereby generating an electrochemical gradient that is used to drive energy-requiring processes such as ATP synthesis and active transport (Dutton, 1986; Prince, 1990).

The cyt bc_1 complex from the Gram-negative, purple nonsulfur photosynthetic bacterium *Rhodobacter capsulatus* is composed of three protein subunits (Robertson et al., 1993) encoded by the structural genes *fbcF*, *fbcB*, and *fbcC* (Daldal et al., 1987; Davidson and Daldal, 1987a,b). Each subunit binds at least one metal-containing prosthetic group. The cyt *b* subunit houses two molecules of protoheme identified as cyt b_L and b_H (according to their relatively high and low E_{m7} values) that are spectrally and electrochemically distinct. Cyt c_1 contains one molecule of *c*-type heme and the "Rieske" iron–sulfur protein binds a [2Fe–2S] cluster. In addition to these cofactors the enzyme has interaction sites for cyt c_2 and ubi(hydro)quinone.

A modified Q-cycle mechanism (Mitchell, 1976; Crofts and Wraight, 1983; Dutton, 1986; Ding et al., 1992) has been used to describe electron transfer and the coupled proton movements through the complex. This model envisions a low- and high-potential chain of electron transfer and two separate, independent sites for quinone interaction. The site of hydroquinone oxidation (Q_o) is likely to be shared between the cyt *b* and the Rieske Fe–S subunits on the periplasmic side

† This work was supported by NIH Grants GM 38237 to F.D. and 27309 to P.L.D. K.A.G. was a recipient of a fellowship from the American Heart Association, Southeastern Pennsylvania Affiliate.

* To whom correspondence should be addressed.

‡ Department of Biology, Plant Science Institute.

§ Department of Biochemistry and Biophysics, Johnson Research Foundation.

® Abstract published in *Advance ACS Abstracts,* January 1, 1994.

[1] Abbreviations: cyt bc_1 complex, ubihydroquinone–cytochrome *c* oxidoreductase; cyt, cytochrome; EPR, electron paramagnetic resonance; cyt b_H, high-potential cytochrome *b*; cyt b_L, low-potential cytochrome *b*; cyt b_{150}, high-potential form of cytochrome b_H; [2Fe–2S], "Rieske" iron–sulfur cluster; E_{m7}, equilibrium oxidation–reduction midpoint potential at pH 7; E_h, ambient redox potential; PMS, *N*-methyldibenzopyrazine methosulfate; PES, *N*-ethyldibenzopyrazine ethosulfate; Q_a, tightly bound primary quinone in the reaction center; Q_b, loosely bound secondary quinone in the reaction center that undergoes a two-electron and two-proton reduction to the dihydroquinone species; PMSF, phenylmethanesulfonyl fluoride; EDTA, ethylenediaminetetraacetic acid; MOPS, (*N*-morpholino)propanesulfonic acid; 3-(maleimidomethyl)-proxyl, 2,2,5,5-tetramethyl-1-pyrrolidinyloxy-3-(maleimidomethyl); BChl, bacteriochlorophyll; SDS–PAGE, sodium dodecyl sulfate–polyacrylamine gel electrophoresis; DBH, 2,3-dimethoxy-5-decyl-6-methyl-1,4-benzohydroquinone; ENDOR, electron nuclear double resonance.

0006-2960/94/0433-723$04.50/0

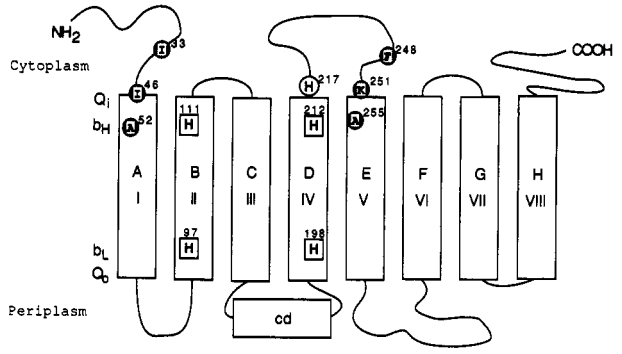

FIGURE 1: Folding model of the cyt *b* polypeptide (Robertson et al., 1990). The four histidines which are the ligands to cyt b_L and b_H are in boxes in helices B (II) and D (IV). Positions in stippled circles are sites of spontaneous mutations which confer resistance to Q_i site inhibitors in mouse and yeast mitochondria. The putative Q_i and Q_o regions are indicated on opposite sides of the membrane. H217 is circled.

of the membrane (Robertson et al., 1986, 1990) while the site of quinone reduction (Q_i) appears to be confirmed to the cyt *b* polypeptide on the cytoplasmic side of the membrane. Oxidation of QH_2 at the Q_o site does not involve a stable semiquinone intermediate; the concerted two-electron oxidation process by the single-electron carriers, the [2Fe–2S] cluster and cyt b_L, requires a low stability of the intermediate semiquinone. In contrast, a stable semiquinone intermediate is readily observed at the Q_i site (Ohnishi and Trumpower, 1980; Robertson et al., 1984b), consistent with its proposed role of accumulating two single electrons from cyt b_H to produce ubihydroquinone in an analogous manner to the Q_b site of the photosynthetic reaction center.

There is no high-resolution crystal structure yet available for a cyt bc_1 complex. Thus structural analysis relies upon a variety of other experimental approaches and molecular modeling. One of the most powerful methods is specific mutagenesis followed by rigorous physicochemical studies. This combination of approaches not only provides structural information but also may address mechanistic questions. Folding models (Figure 1) of the cyt *b* polypeptide based on the primary sequence predict that there are eight transmembrane α-helices and one amphipathic helix (Rao and Argos, 1986; Crofts et al., 1987). The sites of spontaneous mutations which confer resistance to either Q_o or Q_i site-specific inhibitors are localized to either the periplasmic or cytoplasmic sides of the membrane (di Rago et al., 1986, 1989; Howell et al., 1987; di Rago and Colson, 1988; Howell and Gilbert, 1988; Weber and Wolf, 1988; Daldal et al., 1989) supporting the folding models.

Without a crystal structure it is difficult to pinpoint residues that play critical roles in the protein. However, an impressive number of cyt *b* genes have been sequenced (over 700) and sequence alignments [Degli-Esposti et al. (1993) and Figure 2] have shown that there are very few highly conserved residues in the protein. The assumption is that a highly conserved residue performs a vital function, be it structural or functional. Among the seven histidines present in the cyt *b* subunit, five are invariant. Four of these, H111, H212, H97, and H198, appear to be ligands to the two protoheme moieties (b_H and b_L, respectively) (Yun et al., 1991) and are located on putative helix B (II) and D (IV) in positions consistent with the current model, which has cyt b_H close to the cytoplasmic side and cyt b_L near the periplasmic side of the membrane. The fifth highly conserved histidine, H217 (H202 in the numbering from yeast), is predicted to lie near cyt b_H and close to the Q_i site. These reasons led us initally to inquire whether H217 plays a specialized role in the Q_i site of the cyt bc_1 complex.

As can be seen in Figure 2 and the alignments of Degli Esposti et al. (1993), H217 is not conserved in the cyt b_6 subunit from chloroplasts and the cyanobacteria but the homologous position is occupied by arginine. Cyt b_6 is different in several regards from other cytochromes *b*. Cyt b_6 is much shorter and in fact is very closely related to the amino-terminal half of cyt *b*, while subunit IV from the chloroplast complex is more homologous to the carboxyl-terminal half of cyt *b*. The combination of cyt b_6 and subunit IV thus forms a split cyt *b* with the truncation point only a few residues past position 217. In addition, the cyt b_6f complex is insensitive to the Q_i inhibitor antimycin (Hauska et al., 1983) and no stable semiquinone is detectable. Therefore the general architecture of the Q_i site in the cyt b_6f complex may well be different from the cyt bc_1 complex [for reviews see Rich (1986) and Widger and Cramer (1990)] and sequence alignments in this region could be misleading.

In this work we have used site-directed mutagenesis to substitute H217 of the cyt *b* subunit of the cyt bc_1 complex from *R. capsulatus* with various other residues. The mutants were examined in regard to effects on growth, the cyt b_H and Q_i site quinone redox potentials, and time-resolved kinetics of electron transfer involving cyt b_H and the quinone of the Q_i site. The results suggest that H217 is important to the properties of the Q_i site quinone and its interaction with cyt b_H.

MATERIALS AND METHODS

Bacterial Strains and Growth. Escherichia coli strains were grown as described previously (Atta-Asafo-Adjei and Daldal, 1991). *R. capsulatus* was grown by microaerophilic respiration in the dark at 35 °C in rich medium (MPYE) supplemented with 10 μg/mL kanamycin. Cultures were shaken at 150 rpm in a rotary shaker, conditions under which the components of the photosynthetic apparatus (reaction center and light-harvesting complexes) are induced. pMTS1/MT-RBC1 is an *R. capsulatus* strain which overproduces wild-type cyt bc_1 complex. This strain has a chromosomal deletion of the *fbc* operon (Atta-Asafo-Adjei and Daldal, 1991), in which the structural genes of the cyt bc_1 complex have been replaced by a spectinomycin resistance gene, and is complemented in trans by a newly designed plasmid (pMTS1; M. Tokito and F. Daldal, manuscript in preparation). pMTS1 facilitates the subcloning of the *in vitro*-made mutations from the replicative form of phage M13 directly to a conjugation-proficient plasmid. pMTS1 contains a wild-type copy of the *fbc* operon and a kanamycin resistance gene as a marker. Trans complementation results in an approximately 5-fold overproduction of the cyt bc_1 complex when the cells are grown aerobically (Atta-Asafo-Adjei and Daldal, 1991). Mutant *R. capsulatus* strains are referred to by the nature of the substitution at H217; for example, the designations *b*H217D, -R, and -L refer to the strains in which H217 of cyt *b* has been replaced by aspartic acid, arginine and leucine, respectively.

Genetic Techniques. Site-directed mutagenesis was performed as described by Atta-Asafo-Adjei and Daldal (1991) using the uracilated phage M13mp10-BC1*Sma*del6 as template (Gray et al., 1992). The mutagenic oligonucleotide used was petB-H217, 5′-TGG GCC TTC [(G/C)(A/T/G)C] ACC ACC CGG-3′. After mutagenesis and screening by nucleotide sequencing, the petB-H217D (GAC), petB-H217L (CTC), and petB-H217R (CGC) mutations were retained. The *Sma*I/

		H 2 1 2	H 2 1 7
bacterial	R.s.	llpfviaalv	aiHiwafH.t tgnnnptgve vrrtskadae kdtlpfwpyf
	R.c.	llpfviaalv	aiHiwafH.t tgnnnptgve vrrtskadae kdtlpfwpyf
	R.v.	llpfvivgvv	mlHvwalH.v tgqtnptgve vk.....se kdtvrftpfa
	R.r.	lfpmllfavv	flHmwalH.v kksnnplgid ak.....gp fdtipfhpyy
mitochondrial	S.c.	lvpfiiaamv	imHlmalH.i hgssnplgit .....gn ldripmhsyf
	Beef	ilpfiimaia	mvHllflH.e tgsnnptgis .....sd vdkipfhpyy
	Human	ilpfiiaala	tlHllflH.e tgsmmplgit .....sh sdkitfhpyy
	Mouse	ilpfiiaala	ivHllflH.e tgsmmptgln .....sd adkipfhpyy
	Eel	lfpfvvaalt	mlHllflH.e tgsmmpvgln .....sd adkipfhpyf
chloroplast	Spinach b_6	vlplltavfm	lmHflmiRkq gisg.pl. end of cyt b_6
	Nostoc b_6	vlpwliavfm	lfHflmiRkq gisg.pl. end of cyt b_6

FIGURE 2: Sequence alignment of a short stretch of the cyt $b(b_6)$ polypeptide. H212 is a ligand to cyt b_H. R.s., *Rhodobacter sphaeroides*; R.c., *Rhodobacter capsulatus*; R.v., *Rhodopseudomonas viridis*; R.r.; *Rhodospirillum rubrum*; S.c., *Saccharomyces cerevisiae*.

*Asu*II fragment from the replicative form of M13 was exchanged with the corresponding fragment of pMTS1 yielding pMTS1-bH217D, pMTS1-bH217L, and pMTS1-bH217R. The plasmids thus obtained were conjugated into *R. capsulatus* strain MT-RBC1, selecting for kanamycin resistance. Sequences were reconfirmed following plasmid isolation from *R. capsulatus*.

Biochemical Techniques. Cells were ruptured in an Aminco French pressure cell at 16 000 psi in the presence of 1 mM phenylmethanesulfonyl fluoride (PMSF) and 0.5 mM EDTA. Cells were passed through the cylinder twice and the chromatophores were isolated by differential centrifugation as described previously (Atta-Asafo-Adjei and Daldal, 1991).

Redox Titrations. Optical potentiometric titrations were performed as described previously (Dutton, 1978). Chromatophores were suspended to 50 μM bacteriochlorophyll in 50 mM MOPS and 100 mM KCl, pH 7, with the following mediators (with their respective midpoints at pH 7): 25 μM 1,4-benzoquinone (280 mV), 70 μM 2,3,5,6-tetramethyl-*p*-phenylenediamine (240 mV), 25 μM 1,2-naphthoquinone (145 mV), 20 μM *N*-methyldibenzopyrazine methosulfate (PMS) (80 mV), 25 μM 1,4-naphthoquinone (60 mV), 20 μM *N*-ethyldibenzopyrazine ethosulfate (PES) (55 mV), 50 μM duroquinone (5 mV), 20 μM pyocyanine (–30 mV), 25 μM 2-hydroxy-1,4-naphthoquinone (–145 mV), and 20 μM phenazine (–180 mV). Data points (A_{560} minus A_{540}) were normalized and fit to multiple $n = 1$ Nernst equations by varying both the amplitude and E_m value of each component.

EPR titrations of the semiquinone were performed anaerobically in the presence of redox dyes at pH 8.8 as outlined by Dutton (1978). Mediators were 40 μM safranin T (–289 mV), 1,2-naphthoquinone, benzoquinone, indigodisulfonate (–125 mV), duroquinone, phenylsafranin (–252 mV), 1,4-naphthoquinone, and 1,2-naphthoquinone 4-sulfonate (217 mV). The antimycin-sensitive semiquinone ($Q^{\bullet -}$ at Q_i) was assayed using a Varian E-109 X-band spectrometer by measuring the peak to trough amplitude of the $g = 2.005$ derivative signal obtained at 20 μW power and 143 K and was corrected for the residual signal observed in the presence of antimycin (80 μM). The absolute concentration of semiquinone was determined for the sample with the highest signal in each titration by spin quantitation using a spin label, 3-(maleimidomethyl)-PROXYL (courtesy of Dr. T. Ohnishi) as a standard.

Detailed analyses of the thermodynamic properties of the semiquinone from both mitochondria (de Vries et al., 1980; Robertson et al., 1984b) and bacteria (Robertson et al., 1984b; McCurley et al., 1990) demonstrated that the optimum pH for the observation of the semiquinone identified as the semiquinone anion is approximately 9 and that the maximum amount observed per cyt bc_1 complex is about 0.3 for *Rhodobacter sphaeroides* and 0.6 for the beef heart enzyme. A similar analysis has been used here to determine the stability constant of the semiquinone and the $Q/Q^{\bullet -}$ and $Q^{\bullet -}/QH_2$ E_m values in the wild-type and mutant strains.

Time-Resolved Kinetics. Flash-activated single-turnover kinetics were measured as described previously (Robertson et al., 1986) on a dual-wavelength spectrophotometer fitted with an anaerobic redox cuvette (Johnson Foundation Biomedical Instrumentation Group, University of Pennsylvania). Single, short (8-μs) pulses of saturating actinic light were delivered to the cuvette at 90° to the measuring beam. Samples were poised at specific ambient potentials (indicated in the text and figure legends) in the presence of mediators [10 μM 2-hydroxy-1,4-naphthoquinone, 10 μM 2,3,5,6-tetramethyl-*p*-phenylenediamine, 10 μM Fe(III)EDTA, 2 μM PMS, and 2 μM PES] and allowed to come to equilibrium in darkness prior to flash activation. The presence of mediators caused minimal interference with the kinetic measurements.

Inhibitors and the K^+-specific ionophore valinomycin were added when needed and indicated in the figure legends. Kinetics of cyt *b* reduction and reoxidation were measured at 560 *minus* 570 nm, total cyt *c* oxidation and rereduction were measured at 550 *minus* 542 nm, carotenoid band shift was measured at 475 *minus* 490 nm, and $BChl_2$ oxidation was measured at 605 *minus* 540 nm. Reaction center concentration was calculated by adjusting the redox potential to 380 mV followed by a train of eight actinic flashes separated by 32 ms. The extinction coefficient 29 mM^{-1} cm^{-1} and $\Delta A_{605-540}$ were then used to calculate the concentration.

Four basic kinetic measurements were performed to assay cyt b_H and Q_i site function. These are outlined below and shown schematically in the diagrams accompanying Figures 5 and 7. In all cases the redox potential of the chromatophores was adjusted so that the high-potential chain (consisting of cyt c_2, cyt c_1, and the [2Fe–2S]) was reduced and the low-potential chain (consisting of cyt b_L and cyt b_H) was oxidized prior to flash activation. Within this range the redox state of the ubiquinone pool was poised oxidized or partly reduced as described below. In all measurements the experimentally observed components were predominantly cyt b_H and cytochromes $c_1 + c_2$ (henceforth referred to as cyt *c*). Electron transfer through the cyt bc_1 complex is initiated by the microsecond oxidation of cyt c_2 by the photooxidized BChl dimer of the reaction center. This oxidation starts a chain of events marked by the oxidation of QH_2 at the Q_o site by the [2Fe–2S] and cyt b_L.

(1) *Cyt b_H Reduction via QH_2 at the Q_o Site.* The best measure of the first QH_2 oxidized by the Q_o site is provided by observing the rate of cyt b_H reduction in complexes inhibited by antimycin (Robertson et al., 1990; Figure 5, event 2), whereas the second QH_2 oxidized by the Q_o site is displayed by the rereduction kinetics of cyt *c* (Figure 5, event 1). The rate of QH_2 oxidation at the Q_o site is dependent upon the redox state of the Q_{pool}. At relatively high redox potentials (around 200 mV) the Q_{pool} is >99% Q, which after flash activation yields the minimum rate of turnover (Prince et al., 1978; Crofts et al., 1983). However, at lower redox potentials established to partly reduce the Q_{pool} the Q_o site turns over faster; in the experiments reported here the redox potential used was about 100 mV so that the Q_{pool} was about half-reduced prior to flash activation. Thus, by comparing the time courses of cyt b_H reduction in the wild-type and mutant strains following flash activation at both 200 and 100 mV it can be ascertained whether the mutations have affected the rate of arrival of electrons to cyt b_H.

(2) *Cyt b_H Oxidation via the Q_i Site.* Under physiological conditions cyt b_H, reduced by QH_2 via the Q_o site, is reoxidized by Q bound to the Q_i site. Thus at relatively high redox potentials (200 mV) when the Q_o site turns over slowly, very little stable reduced cyt b_H is evident. In contrast, at lower potentials (100 mV) both reduction and reoxidation kinetics can be observed. Thus, by noting either the amount of stable reduced cyt b_H at high potentials or the rate of b_H reoxidation at lower potentials the activity of the Q_i site can be assayed.

(3) *QH_2 Oxidation at the Q_i Site.* At alkaline pH values and in the presence of the Q_o site inhibitor myxothiazol, it has been demonstrated that it is both thermodynamically and kinetically feasible for QH_2 at the Q_i site to reduce cyt b_H (Glaser et al., 1984; Robertson et al., 1984a; Figure 7, event 3). The details of the reaction are unclear, but it appears to be either an equilibration of QH_2 in the pool with cyt b_H or a direct interaction of Q_b with cyt b_H. We took advantage of this pathway of electron transfer between QH_2 at the Q_i site and cyt b_H to compare the rates and extents of cyt b_H reduction in the wild-type and mutant strains.

(4) *Electrochromic Carotenoid Band Shift.* Flash-induced charge separation across the low dielectric of the chromatophore membrane establishes a membrane electrical potential which perturbs the electronic properties of the light-harvesting carotenoids resulting in a red shift in their absorption spectra (Jackson and Crofts, 1969). Electron transfer through both the reaction center and the cyt bc_1 complex is electrogenic (Jackson and Dutton, 1973), giving rise to three distinct phases, phases I and II associated with electron transfer through the reaction center and phase III through the cyt bc_1 complex. It has been further demonstrated (Glaser and Crofts, 1984; Robertson and Dutton, 1988) that the events responsible for phase III are electron transfer from cyt b_L to cyt b_H (myxothiazol-sensitive) and between cyt b_H and quinone bound at the Q_i site (antimycin-sensitive). Therefore, by monitoring the antimycin-sensitive component of the flash-induced carotenoid band shift, information complementary to the cytochrome redox changes is obtained.

Chemicals. PMS, PES, 2-hydroxy-1,4-naphthoquinone, benzoquinone, Fe(III)EDTA, phenazine, 1,2-naphthoquinone disulfonate, 3-(maleimidomethyl)-PROXYL, Type VI horse heart cytochrome *c*, valinomycin, and antimycin were purchased from Sigma Chemical Co. (St. Louis, MO). 1,2-Naphthoquinone, 2,3,5,6-tetramethyl-*p*-phenylenediamine, duroquinone, and 1,4-naphthoquinone were purchased from Aldrich Chemical Co. (Milwaukee, WI). Safranin T, indigodisulfonate, and phenylsafranin were purchased from Fluka Chemika AG (Buchs, Switzerland). Pyocyanine was a kind gift from Dr. D. E. Robertson, University of Pennsylvania. Myxothiazol was purchased from Boehringer-Mannheim Biochemicals. All other chemicals were reagent grade and were purchased from commercial sources.

RESULTS

Growth Properties. Photosynthetic competency of the wild-type and mutant strains was tested both in liquid culture and on plate. It has been demonstrated that a functional cyt bc_1 complex is required for phototrophic growth in *R. capsulatus* (Daldal et al., 1987) and it was observed that both *b*H217D and R are able to grow photoheterotrophically with doubling times in rich medium of approximately 300 and 360 min, respectively (compared to about 120 min for the wild-type strain, pMTS1, overproducing the cyt bc_1 complex). However, *b*H217L is unable to grow anaerobically in the light. Spontaneous photosynthetic revertants of *b*H217L could be isolated (at a frequency of 10^{-6}) and nucleotide sequence analysis of plasmids from four independent revertants showed that the reversion took place at the site of the original mutation, and all reverted back to wild type (CAC).

Subunit, Heme Group Content, and Cyt c Reductase Activity. SDS–PAGE analysis (not shown) of chromatophore membranes indicated that all mutants contain the three subunits of the cyt bc_1 complex. Furthermore, redox difference spectra (dithionite-reduced *minus* ascorbate/PMS-reduced and ascorbate/PMS-reduced *minus* ferricyanide-oxidized) showed that all three mutants have similar amounts of ascorbate-reducible cyt *c* and dithionite-reducible cytochrome *b* in the membrane. Neither SDS–PAGE nor redox difference spectra suggested that there is any substantial variation in amounts of the complex between various strains.

Chromatophore fractions of strains containing the mutant plasmids were assayed for cyt *c* reductase activity using the nonphysiological ubihydroquinone analog 2,3-dimethoxy-5-decyl-6-methyl-1,4-benzohydroquinone (DBH) as electron donor and equine ferricytochrome *c* as electron acceptor. The steady-state turnover kinetics mimicked the growth properties described above; *b*H217D and -R had approximately 60% while *b*H217L had only 10% of the wild-type activity [wild-type chromatophores in this instance had a steady-state turnover of 3536 nmol of cyt *c* reduced min^{-1} (mg of membrane protein)$^{-1}$].

Redox Titrations. Potentiometric titrations were performed at pH 7 in the presence and absence of antimycin to determine whether the mutations affected the thermodynamic properties of cyt b_H and b_L. Typical titrations are shown in Figure 3 and the midpoints are summarized in Table 1. In wild type (that is, the cyt bc_1 overproducer in this work) chromatophores, cyt b_L and cyt b_H titrate with midpoint potentials of −111 and 51 mV, respectively. Within the limits of the measurements (±15 mV) these values agree with previous reports using chromatophores from *R. capsulatus* (Robertson et al., 1986). A third component with an E_m of 138 mV was used in the fitting procedure to obtain the best fit to the data. This component, referred to as cyt b_{150}, has been noted before (Berden and Opperdoes, 1972; Dutton and Jackson, 1972) and appears to be a high-potential form of cyt b_H thought to result from a redox interaction between the quinone bound at the Q_i site and b_H (de la Rosa and Palmer, 1983; Salerno et al., 1989; Rich et al., 1990). A titration of chromatophores lacking the cyt bc_1 complex (derived from the strain MT-RBC1) showed no feature with an E_{m7} value around 150 mV (data not shown),

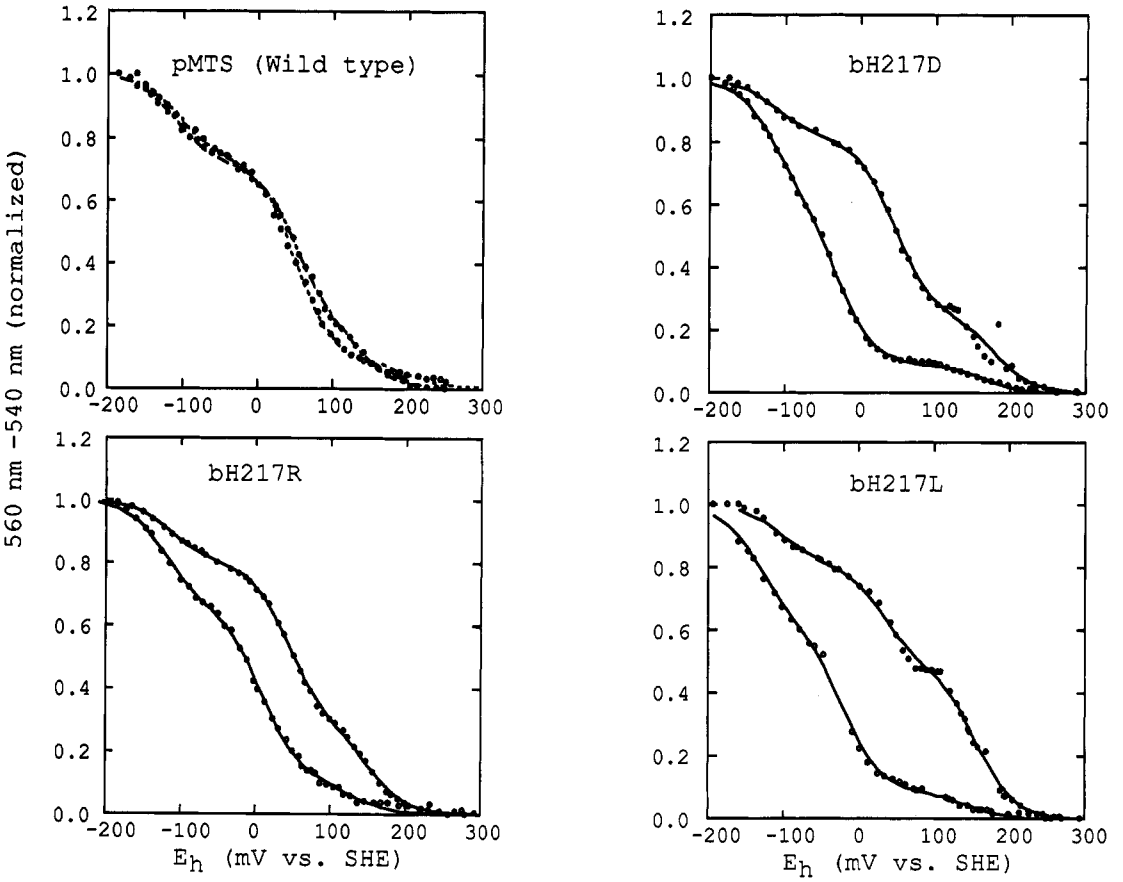

FIGURE 3: Redox titrations of chromatophore fractions from the wild-type (pMTS1) and mutant strains used in this study. Chromatophores (50 μM in BChl) were suspended in 50 mM MOPS, pH 7, containing 100 mM KCl and redox mediators indicated in the text. The wavelength pair 560 minus 540 nm was used to monitor the redox state of the *b*-type hemes. The closed circles represent data points in the absence of any inhibitor, while the open circles are in the presence of antimycin (20 μM). The data were fit to multiple $n = 1$ Nernst equations (shown in solid lines) with the E_m values and amplitudes of the fits detailed in Table 1.

Table 1: E_{m7} Values and Fit Amplitudes (A) in the Absence and Presence (20 μM) of Antimycin for Each of the *b* Hemes from Wild Type (pMTS1) and H217 Mutants[a]

	E_{m7} (mV)					
	no additions			+ antimycin		
strain	b_L (A)	b_H (A)	b_{150} (A)	b_L (A)	b_H (A)	b_{150} (A)
pMTS1	−111 (0.28)	51 (0.51)	138 (0.2)	−105 (0.3)	51 (0.7)	none
*b*H217D	−114 (0.18)	45 (0.57)	180 (0.25)	−117 (0.36)	−32 (0.55)	167 (0.09)
*b*H217R	−114 (0.2)	44 (0.51)	152 (0.29)	−121 (0.35)	9 (0.55)	131 (0.1)
*b*H217L	−103 (0.18)	32 (0.33)	156 (0.48)	−132 (0.38)	−22 (0.53)	146 (0.08)

[a] Values were derived from the fits shown in Figure 3. Experimental conditions are in Materials and Methods.

lending support to the proposal that cyt b_{150} is specific to the cyt bc_1 complex. As shown in Table 1, titrations of the mutants show only minor variations in E_{m7} values from the native values, but cyt b_{150} accounts for a higher percentage of the total cyt *b* in all mutants, with the most dramatic effect seen in *b*H217L, in which about 50% has an E_{m7} value of 156 mV. Plots of the absorption changes (not shown) at various ambient redox potentials show that the spectrum of cyt b_{150} appears identical to that of ferrocytochrome b_H with a single maximum in the α band at 560 nm.

Also shown in Figure 3 are titrations performed in the presence of antimycin (open circles). When antimycin is bound to the Q_i site of the wild-type enzyme, cyt b_{150} reverts to the 50 mV titrating form of cyt b_H, similar to that observed when antimycin is bound to the Q_i site of mitochondrial cyt bc_1 complex (Rich et al., 1990). In contrast to the situation in wild-type chromatophores, the binding of antimycin severly perturbs the redox behavior of cyt b_H in all three mutant strains. Thus the binding of antimycin confers a large stabilizing effect on the oxidized state of cyt b_H and removes most of the species responsible for cyt b_{150}. An apparent increase in the contribution of cyt b_L after antimycin binds to the Q_i site in the mutants is also seen (Table 1). This may suggest that some cyt b_{150} also arises form cyt b_L; however, the contributing cyt b_{150} is rather spectrally similar to cyt b_H and not cyt b_L. Comparison of the absorption spectra taken at various redox potentials indicates that the increased amplitude of the low-potential titrating cyt *b* is due to a contribution of cyt b_H at these potentials. This indicates that when antimycin binds at the Q_i site of the mutants the redox behavior of cyt b_H is more complex than suggested by the fits and that there may be multiple electrochemical forms of cyt b_h under these conditions.

In addition to the determination of the E_m values of cytochromes b_H and b_L, the redox properties of quinone bound at the Q_i site have been measured at an optimal pH.

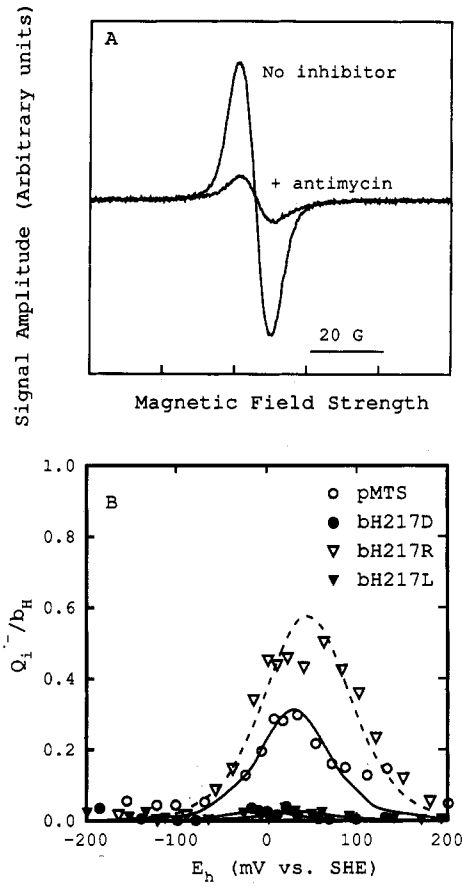

FIGURE 4: Redox titrations of the antimycin-sensitive semiquinone in chromatophores of pMTS1 and H217 mutants at pH 8.8. Chromatophores were suspended in 150 mM glycine, pH 8.8, containing 100 mM KCl and redox dyes indicated in the text. (A) $g = 2.00$ radical signal observed in wild-type chromatophores in the absence ($E_h = 60$ mV) and presence ($E_h = 62$ mV) of antimycin. (B) The data points represent normalized peak to trough $g = 2.00$ signal corrected for the residual signal present after antimycin was added. The curves are fits to the data using the assumption that there is one Q_i site per cyt bc_1 complex.

Chromatophores isolated from pMTS1 displayed a redox potential dependency of the antimycin-sensitive free radical (Figure 4A), which indicates that the E_m values of $Q/Q^{\bullet-}$ and $Q^{\bullet-}/QH_2$ are both around 29 mV at pH 8.8 and a maximal amount of $Q^{\bullet-}$ per cyt b_H of 0.3 is observed (Figure 4B). Using the same analysis as Robertson et al. (1984b), these numbers indicate that the stability constant (K_{STAB}) for the semiquinone at this pH is close to 1. Under the same conditions a much larger signal was observed in *b*H217R, $Q^{\bullet-}$ per cyt $b_H = 0.6$, with E_m values for $Q/Q^{\bullet-}$ and $Q^{\bullet-}/QH_2$ of 75 and 15 mV, respectively. Thus K_{STAB} for the semiquinone in *b*H217R is close to 10 at this pH. The other two strains had very small antimycin-sensitive signals (*b*H217D, $Q^{\bullet-}$ per cyt $b_H = 0.03$, *b*H217L, $Q^{\bullet-}$ per cyt $b_H = 0.025$) and fits to the data result in E_m values for $Q/Q^{\bullet-}$ and $Q^{\bullet-}/QH_2$ of −72 and 70 mV for *b*H217D and −12 and 125 mV for *b*H217L. These numbers in each mutant demonstrate an unstable $Q^{\bullet-}$ with a K_{STAB} of 5×10^{-3} for both. It is important to add however, that these fits are based on the assumption that the full complement of quinone is still bound at the site. At present we have no way of determining Q_i site occupancy by Q or QH_2 and hence the apparently low K_{STAB} could arise because only a small population of bound quinone is present in the Q_i site.

Flash-Activated Single Turnover Kinetics: (*A*) *Effects of the Mutations on Cyt b_H Kinetics.* The growth and steady-state turnover defects in the mutant strains described above suggest that electron transfer rates in the mutant cyt bc_1 complexes have been decreased. Results obtained by monitoring cyt *b* reduction after flash activation of chromatophores poised at an ambient potential of 180 mV are shown in Figure 5. Very little stable reduced cyt b_H (approximately 20% of the total) is observed after the flash in uninhibited wild-type chromatophores (Figure 5A). In contrast, both *b*H217D and -R show substantial reduction of cyt b_H (almost 100% of the total). Point spectra of the absorbance changes from 540 to 580 nm taken 20 ms after the flash at this potential (data not shown) verify that the reduced species is cyt b_H ($\lambda_{max} = 560$ nm) in these strains. The extent of cyt *b* reduction in *b*H217L is similar to wild type, but the point spectrum has a split peak ($\lambda_1 = 566$ nm, $\lambda_2 = 560$ nm) suggesting that the reduction is dominated by cyt b_L and not b_H. All strains display essentially the same rates between 150 and 240 s^{-1} of cyt b_H reduction when antimycin is bound to the Q_i site (Figure 5B, Table 2). As expected, the addition of the Q_o-specific inhibitor myxothiazol blocks the reduction of cyt *b* in all samples (not shown).

In chromatophores poised at 100 mV the wild type displays the expected enhanced rate of flash-induced cyt b_H reoxidation (Figure 5C). In contrast, rates of flash-induced cyt b_H reoxidation in *b*H217D and -R are much slower. The data obtained from *b*H217L are anomalous as described for work done at 180 mV. Again very little flash-induced reduction of cyt *b* occurs and a point spectrum of the absorbance changes show only reduced cyt b_L. In order to estimate the reoxidation rates of cyt b_H in the various samples, a difference was taken between traces obtained with and without the antimycin (Figure 5C,D). The resultant kinetic trace was then fit to an exponential equation and the rates obtained are summarized in Table 2. In wild-type chromatophores cyt b_H is reoxidized at a rate of approximately 300 s^{-1}. However, it is not possible to satisfactorily fit the *b*H217D data to a single exponential but a biphasic fit results in two rates, $k_1 = 10$ s^{-1} and $k_2 = 200$ s^{-1} (with amplitudes of 0.6 and 0.4, respectively). In contrast, the data from *b*H217R can be fit to a single-exponential decay giving a rate of 90 s^{-1}, a value that is about 3-fold slower than wild type.

(*B*) *Effects of the Mutations on Cyt c Kinetics.* At redox potentials near 180 mV the rate of cyt *c* reduction is approximately 35 s^{-1} in the wild type (Figure 6A and Table 2). Both *b*H217D and *b*H217R are slowed 2-fold (15 s^{-1}) but no detectable rereduction of cyt *c* is apparent in chromatophores of *b*H217L. When antimycin binds to the Q_i site (Figure 6B) the kinetics of wild type and *b*H217D and -R are affected in a similar manner, but *b*H217L is unperturbed by the inhibitor, suggesting that the uninhibited enzyme behaves as if electron transfer through the cytochromes b_L and b_H is already inhibited. All strains are sensitive to myxothiazol (data not shown). The results obtained at 100 mV (Figure 6C,D) are qualitatively the same as those at higher redox potentials, the only difference being the increased rate of cyt *c* rereduction in all samples (to around 350 s^{-1} in wild-type chromatophores). The decreased rate of cyt *c* rereduction in the mutant chromatophores is less apparent at this redox potential (slowed to less than a factor of 2 in both H217D and -R) than at 180 mV.

(*C*) *Effects of the Mutants on the Reduction of Cyt b_H via the Q_i Site.* Cyt b_H in wild-type chromatophores (poised at $E_h = 120$ mV) is reduced by QH_2 at the Q_i site at a rate of about 200 s^{-1} (Figure 7 and Table 2). The rate is about 16 s^{-1} in *b*H217D, 9 s^{-1} in *b*H217R, and undetectable in *b*H217L. The extent of cyt b_H reduction, however, in *b*H217R is about

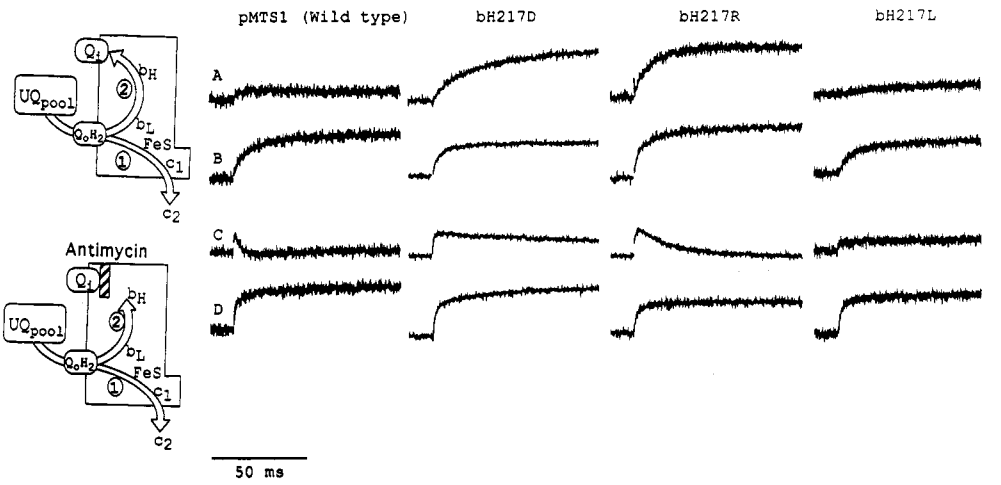

FIGURE 5: Flash-activated absorbance changes of cyt *b* in chromatophores of wild-type (pMTS1) and *b*H217 mutant strains. Chromatophores were suspended to approximately equal concentrations of photobleachable reaction center (0.2 μM) in 50 mM MOPS, 100 mM KCl, pH 7, and 6 μM valinomycin and mediators indicated in the text. The wavelength pair 560 minus 570 nm was monitored after a short (8-μs) saturating (90%) xenon flash. (A) Ambient potential adjusted to 180 mV. (B) Same as (A) except plus 10 μM antimycin. (C) Ambient potential adjusted to 100 mV. (D) Same as (C) except plus 10 μM antimycin. Rates derived from these traces are shown in Table 2. To the left of the traces are schematics representing the electron transfer events being measured. The event labeled (2) is electron transfer from QH_2 to cyt b_H. Antimycin inhibits the reoxidation of cyt b_H by displacing Q from the Q_i site.

Table 2: Rates Derived from the Traces shown in Figures 5–7[a]

residue substitution	total cyt *c* reduction		cyt b_H reduction, Q_{pool} oxidized		cyt b_H oxidation (no addition minus 10 μM antimycin)
	Q_{pool} reduced	Q_{pool} oxidized	$Q_o \rightarrow$ cyt b_H	$Q_i \rightarrow$ cyt b_H	cyt $b_H \rightarrow Q_i$
none (wt)	350	35	150	200	333
*b*H217D	300	15	155	16	$k_1 = 10$, $k_2 = 200$
*b*H217R	239	15	240	9	90
*b*H217L	none	none	181	none	NA

[a] Data points were fit to an exponential equation, and the numbers correspond to the rates (s^{-1}).

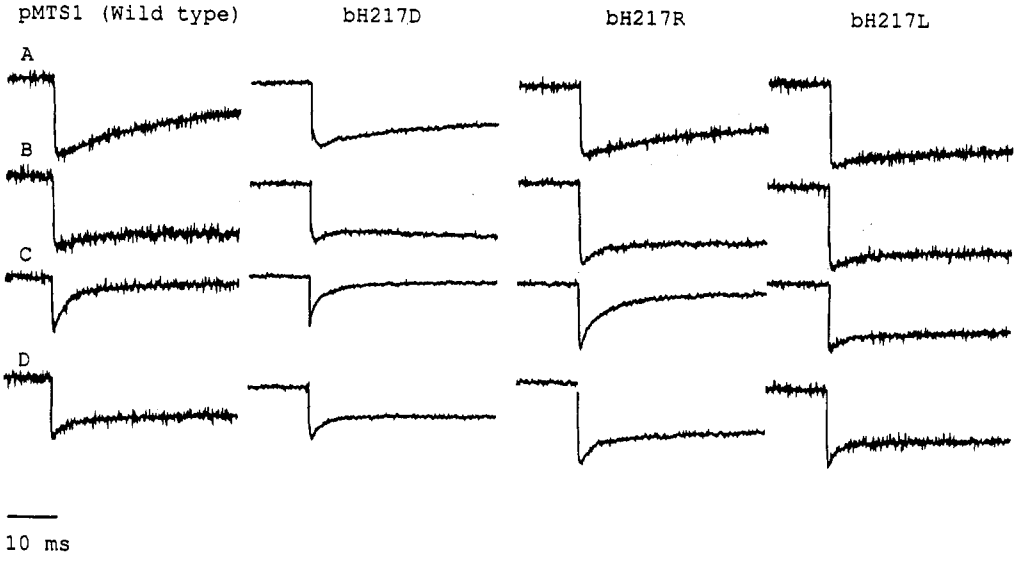

FIGURE 6: Flash-activated absorbance changes of cyt *c* in chromatophores of wild-type (pMTS1) and H217 mutant strains. Conditions are the same as in Figure 5 except that the wavelength pair 550 nm minus 542 nm was monitored. (A) Ambient potential adjusted to 180 mV. (B) Same as (A) except plus 10 μM antimycin. (C) Ambient potential adjusted to 100 mV. (D) Same as (C) except plus 10 μM antimycin. Rates derived from these traces are shown in Table 2. The event labeled (1) in Figure 5 is electron transfer through the cytochromes *c*.

half that of wild type and *b*H217D. As expected, the addition of antimycin abolishes the reduction of cyt b_H in all samples (not shown).

(*D*) *Effects of the Mutations* on the *Electrochromic Carotenoid Band Shift*. Figure 8A shows the flash-induced electrochromic band shift in chromatophores from pMTS1 (Q_{pool} oxidized, E_h = 180 mV) in the absence of any inhibitor and in the presence of either antimycin or myxothiazol. These data are essentially identical to results obtained using chromatophores of *R. sphaeroides* (Robertson and Dutton, 1988). Only the antimycin-sensitive component of phase III is shown in Figure 8, panels B (E_h = 180 mV) and C (E_h = 100 mV). Chromatophores from *b*H217D and *b*H217R have smaller antimycin-sensitive components when poised at 180 mV as compared to the wild type, which correlates well with the observation that flash-induced cyt b_H reoxidation via the

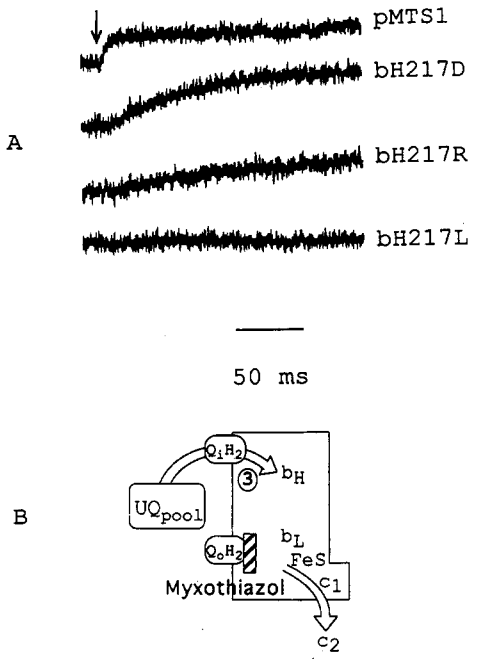

FIGURE 7: (A) Flash-activated Q_i-mediated reduction of cyt b_H in chromatophores of wild-type (pMTS1) and H217 mutant strains. Conditions were as in Figure 5 except that the solution was buffered with 50 mM glycine, pH 9.5, myxothiazol was added to 5 μM, and E_h = 120 mV. The arrow indicates the flash point and the strains are listed to the side. Rates derived from these traces are shown in Table 2. (B) Schematic of the electron transfer event being measured under these conditions (labeled 3).

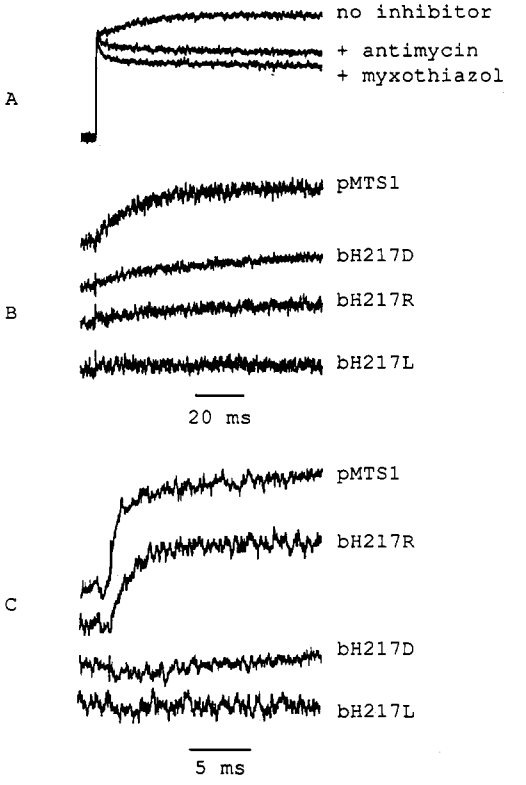

FIGURE 8: (A) Flash-induced carotenoid band shift kinetics in chromatophores of *R. capsulatus* strain pMTS1 at pH 7, E_h = 180 mV. Conditions were as in Figure 5 except that valinomycin was omitted. The wavelength pair 475 minus 490 nm was monitored. Where indicated, antimycin was added to 10 μM and myxothiazol to 5 μM. (B) Antimycin-sensitive component resulting from the subtraction of absorption changes in the presence of antimycin from the absorption changes in the absence of antimycin in the wild-type and mutant strains. (C) Same as (B) except that the redox potential was poised at 100 mV. Note the difference in the time scales between the two measurements.

Q_i site is slowed in these mutants (Figure 5A, above). On the other hand there are only minor differences with and without antimycin in the flash-induced band shift of *b*H217L chromatophores, as expected if electron transfer between cyt b_L and cyt b_H/Q_i is blocked. At redox potentials near 100 mV the rate of the electrochromic band shift increases, similar to the enhanced rate of cyt *b* reduction at this redox potential shown in Figure 5 (note the difference in the time scales between panels B and C in Figure 8). Figure 8C shows that the rate of the antimycin-sensitive component of phase III is slower in the mutants than the wild type and that this rate is slower in *b*H217D than *b*H217R, consistent with the observation that cyt b_H is oxidized more slowly in the former mutant at this potential (Figure 5C). Approximately the same myxothiazol-sensitive component is present in the mutants and wild types (not shown).

In summary, the flash-induced optical changes demonstrate that mutations of H217 deleteriously affect electron transfer between cyt b_H and the ubi(hydro)quinone bound at the Q_i site while the rate of reduction of cyt b_H by QH_2 at the Q_o site is essentially the same as native. This is consistent with the photosynthetic growth of the mutants.

DISCUSSION

In this work three mutants at H217 of the cyt *b* polypeptide were constructed, *b*H217D, -R, and -L. More than one substitution was made with the hope that the observed responses could be correlated with the chemical properties of the substituted side chain and, by extrapolation, the molecular role of the imidazole group of histidine. Imidazole can act as both a hydrogen-bond donor and acceptor, thus making it one of the most versatile amino acid side chains. Although in aqueous solution the side chain has a p*K* near physiological pH, the value could be quite different buried within a protein. A leucine substitution would insert a hydrophobic aliphatic group at this position and remove the potential to form a hydrogen bond. The guanidinium group of arginine has a p*K* of 12.5 and thus it would be expected in an aqueous environment to be positively charged under all experimental and physiological conditions; however, in the protein it has the potential to act as a hydrogen-bond donor and acceptor. In contrast, the carboxyl group of aspartic acid has a p*K* of 3.9 in aqueous solution but again this value could be different within a protein depending upon the electrostatic environment [e.g., E212 of the L subunit in the reaction center has a p*K* around 9 (Paddock et al., 1989, 1990; Takahashi and Wraight, 1990, 1992)] and hence could exist in the protein as the neutral acid or an anion. The hydrogen-bonding ability also depends upon the ionization state of the side chain.

The different mutations had variable phenotypic effects. The insertion of the uncharged, hydrophobic leucine abolishes photosynthetic growth, and steady-state turnover measurements indicate that the enzyme is functionally impaired. The other two substitutions do not abolish growth but do increase the doubling times, with *b*H217R growing more slowly than *b*H217D. Steady-state rates of cyt *c* reduction in these strains are approximately 60% of the native level. Single-turnover kinetic analyses revealed that the rate of electron transfer between the Q_i site quinone and cyt b_H decreases substantially in chromatophores from *b*H217D and -R. In contrast, the reduction of cyt b_H by QH_2 via the Q_o site proceeds virtually unhindered. Interestingly, electron transfer in the nonphysiological direction (from the Q_i site to cyt b_H) occurs both faster and more completely in *b*H217D than in *b*H217R, while

the opposite is true in the physiological direction. The difference between rates of electron transfer observed for mutants in these two pathways may reflect redox equilibria between various intermediates in the reactions. A simple interpretation of the overall kinetic data is that in the wild type the local environment around H217 must be slightly polar since a nonpolar substitution has such dramatic effects while the two polar substitutions have much less of an overall effect.

In all three mutants we observe a larger contribution of the high-potential (cyt b_{150}) form of cyt b_H in the redox titrations. Hacker et al. (1993) have observed similar results in several other Q_i site mutants. It has been suggested (de la Rosa and Palmer, 1983; Salerno et al., 1989; Rich et al., 1990) that cyt b_{150} may result from a redox interaction between a single cyt b_H species and the hydroquinone/semiquinone occupant of the Q_i site. Rich et al. (1990) have shown in submitochondrial particles that there is a larger contribution from cyt b_{150} as the pH of the medium is increased and that it is absent when the Q_i-specific inhibitor antimycin binds the complex. Thus if the redox behavior of the quinone at the Q_i site has been altered by the mutations at H217 one may expect to see variations in the E_m value as well as in the relative contribution of cyt b_{150}. Our observations of increased amounts of cyt b_{150} in the mutants and the large negative shift and variability in the E_m value of cyt b_H after binding antimycin demonstrate that the coupling between quinone bound at the Q_i site and cyt b_H is severely affected by removing H217 and suggest that H217 forms part of the binding pocket of the quinone.

The kinetic and thermodynamic data indicate that the properties of the quinone moiety bound at Q_i have been altered by the substitutions. This could be due to either a binding effect or a perturbation of the electron transfer equilibrium between cyt b_H and Q_i (or a combination of both). These possibilities were addressed by measuring the thermodynamic properties of the $Q/Q^{\bullet -}$ and $Q^{\bullet -}/QH_2$ present at the Q_i site in each of the strains. A positive charge (R) at position 217 serves to increase the stability of the semiquinone over that of the wild type [note that a 60-mV positive shift in the E_m of the $Q/Q^{\bullet -}$ relative to the E_m of the $Q^{\bullet -}/QH_2$ couple translates into an increase of the stability constant of the semiquinone by a factor of 10 (Clark, 1960)]. On the other hand, the insertion of either a negative charge (D) or an aliphatic group (L) strongly destabilizes the semiquinone, yielding a stability constant lower than the wild type. It is interesting that we observe a large amount of cyt b_{150} in a mutant with no detectable semiquinone (H217L), while in a mutant with a highly stable semiquinone we observe only a minor increase in the amount of cyt b_{150} (H217R). This observation appears contrary to the proposals (Rich et al., 1990; de la Rosa et al., 1983; Salerno et al., 1989) which correlated the occurrence of cyt b_{150} with the presence of a stable *semiquinone* bound at the site. However, it is clear that a principal effect of H217 is to influence the redox properties of the Q_i site so that efficient electron transfer between cyt b_H and quinone may occur. The specific effect of the mutations is then on the redox chemistry of quinone at the Q_i site since kinetic defects occur in either increased (R) or decreased (D) semiquinone stability. It is also possible that structural perturbations accompany the thermodynamic changes by *generally* weakening the binding of quinone, which could then contribute to the decreased rate of electron transfer between cyt b_H and the quinone.

The data obtained with *b*H217L do not immediately lend themselves to the same explanation as the other two mutants. Based upon the point spectra and the cyt *c* kinetics, cyt b_H reduction is not observed in uninhibited chromatophores but is observed only after the addition of antimycin. One reason for the different behavior might be the large amount of cyt b_{150} in this strain. Thus at a redox potential of 100 mV, a large amount of cyt b_H (i.e., cyt b_{150}) will be prereduced before flash activation and hence further reduction is not possible. However this is not completely satisfying since at 180 mV there should be sufficient cyt $b_{H(150)}$ oxidized prior to the flash. When antimycin is added there is a large negative shift in the midpoint of cyt b_H and cyt b_{150} (see Figure 3) so at both potentials cyt $b_{H(150)}$ starts oxidized and is reduced following the flash. There may be nonspecific stereochemical and conformational changes caused by leucine which make interpretation more complex. It should be noted that similar kinetic data were observed with a *b*H217A mutant constructed in *R. sphaeroides* by Hacker et al. (1993).

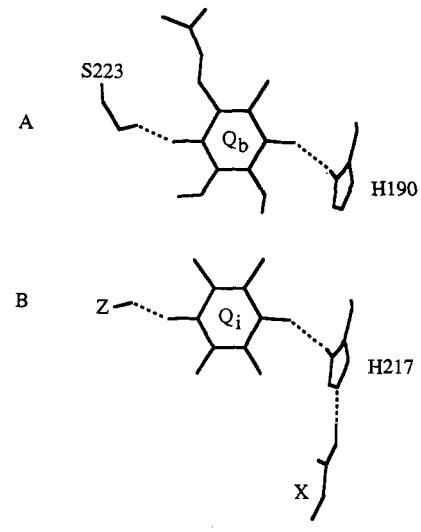

FIGURE 9: (A) Q_b site of the photosynthetic reaction center from *Rhodobacter sphaeroides* (Allen et al., 1988). For simplicity only one isoprenoid unit is shown. (B) Proposed model for the interaction of H217 with quinone bound at Q_i. The quinone methoxy and isoprenoid groups are omitted since the orientation of the ring is not known. X represents another side chain (perhaps from D252 or the heme propionate from cyt b_H) which could hydrogen-bond with H217. Z represents a third residue hydrogen-bonding to the second quinone carbonyl.

The clearly demonstrated involvement of H217 in the activity of the Q_i site prompted us to speculate on the catalytic role of this residue. In the photosynthetic reaction centers from *Rhodopseudomonas viridis* and *R. sphaeroides* histidines (H219 of the M subunit and H190 of the L subunit) are involved in binding quinone at both Q_a and Q_b (Deisenhofer et al., 1984, 1985; Michel et al., 1986; Allen et al., 1988). Furthermore a histidine (H82) has been implicated in quinone binding in fumarate reductase from *E. coli* (Weiner et al., 1986; Westerberg et al., 1990). We suggest that H217 hydrogen-bonds to the quinone carbonyl (Figure 9) reminiscent of the interaction between H190 of the L subunit in the reaction center and the Q_b quinone. The Q_b site is probably a better model than the Q_a site for the Q_i site since similar redox chemistry—two one-electron transfer reactions and the addition of two protons—occurs at both sites. Recent ENDOR data (Salerno et al., 1990) have suggested that the semiquinone species bound at the Q_i site interacts with the protein via hydrogen bonds and that the protons of these bonds are exchangeable with the medium. Salerno et al. (1990) suggest that these hydrogen-bonding interactions could be strong enough to account for the stabilization of the semiquinone, thereby modulating the thermodynamic properties of the

bound quinone. Thus, changing the hydrogen-bonding patterns and the electrostatic environment around the quinone would alter its thermodynamic properties at the site. Further, it may be possible that the second nitrogen of the imidazole ring of H217 is involved in a hydrogen-bonding network that may ultimately provide a pathway for protons to the Q_i binding pocket. Alternatively, the second nitrogen would perhaps hydrogen-bond to one of the heme propionates of cyt b_H, thus providing a direct link between the quinone bound at the Q_i site and the heme. Such a histidine–propionate interaction occurs in myoglobin, where H93 coordinates the heme Fe and H97 hydrogen-bonds to the propionate (Kuriyan et al., 1986). The pair of histidines in cyt *b*, H212/H217, could be acting similarly to the H93/H97 pair in myoglobin. In effect, this model is a chimera of the reaction center Q_b pocket and the myoglobin heme binding pocket. Therefore, breaking these interactions by inserting amino acids which cannot effectively hydrogen-bond to the propionate group and the quinone carbonyl could have effects on both the quinone *and* heme b_H. This may account for the larger amount of cyt b_{150} in those mutants with no measurable semiquinone (especially the leucine substitution); the increased amount of cyt b_{150} would not be due necessarily to a quinone/cyt b_H interaction but to the change in the electrostatic environment around the propionate. Such an arrangement differs from the reaction center in two ways. First, H190 not only binds to ubiquinone at Q_b but also serves as a ligand to the non-heme Fe present between the two quinone binding sites. A similar interaction probably does not occur in the cyt *b* subunit since it is clear from mutagenesis that H212 and H111 are the ligands to the heme Fe of cyt b_H (Yun et al., 1991). Second, H190 does not appear to be important in protonation of the Q_b quinone but other groups (namely, glutamate, aspartate, and serine residues) serve this function (Paddock et al., 1989, 1990; Takahashi and Wraight, 1990, 1992). Further work is needed to learn how similar or dissimilar the two sites are with respect to structure and mechanism.

ACKNOWLEDGMENT

We thank Drs. Dan Robertson and Huangen Ding for many helpful discussions, Dr. Ramy Farid for help with Figure 9, and Mariko Tokito for the construction of the mutants.

REFERENCES

Allen, J. P., Feher, G., Yeates, T. O., Komiya, H., & Rees, D. C. (1988) *Proc. Natl. Acad. Sci. U.S.A. 85*, 8487–8491.

Atta-Asafo-Adjei, E., & Daldal, F. (1991) *Proc. Natl. Acad. Sci. U.S.A. 88*, 492–496.

Berden, J. A., & Opperdoes, F. R. (1972) *Biochim. Biophys. Acta 267*, 7–14.

Clark, W. M. (1960) in *Oxidation and Reduction Potentials for Organic Systems*, Williams and Wilkins Co., Baltimore, MD.

Cramer, W. A., & Knaff, D. B. (1990) in *Energy Transduction in Biological Membranes* (Cantor, C. R., Ed.) Springer-Verlag, New York.

Crofts, A. R., & Wraight, C. A. (1983) *Biochim. Biophys. Acta 726*, 149–185.

Crofts, A. R., Meinhardt, S. W., Jones, K. R., & Snozzi, M. (1983) *Biochim. Biophys. Acta 723*, 202–218.

Crofts, A. R., Robinson, H., Andrews, K., van Doren, S., & Berry, E. (1987) in *Cytochrome Systems: Molecular Biology and Bioenergetics* (Papa, S., Chance, B., Ernster, L., & Jaz, J., Eds.) pp 617–624, Plenum Press, New York.

Daldal, F., Davidson, E., & Cheng, S. (1987) *J. Mol. Biol. 195*, 1–12.

Daldal, F., Tokito, M. K., Davidson, E., & Faham, M. (1990) *EMBO J. 8*, 3951–3961.

Davidson, E., & Daldal, F. (1987a) *J. Mol. Biol. 195*, 13–24.

Davidson, E., & Daldal, F. (1987b) *J. Mol. Biol. 195*, 25–29.

de la Rosa, F. F., & Palmer, G. (1983) *FEBS Lett. 163*, 140–143.

Degli Esposti, M., De Vries, S., Crimi, M., Ghelli, A., Patarnello, T., & Meyer, A. (1993) *Biochim. Biophys. Acta 1143*, 243–271.

Deisenhofer, J., Epp, O., Miki, K., Huber, R., & Michel, H. (1984) *J. Mol. Biol. 180*, 385–398.

Deisenhofer, J., Epp, O., Miki, K., Huber, R., & Michel, H. (1985) *Nature 318*, 618–624.

de Vries, S., Berden, J. A., & Slater, E. C. (1980) *FEBS Lett. 122*, 139–143.

di Rago, J. P., & Colson, A.-M. (1988) *J. Biol. Chem. 263*, 12564–12570.

di Rago, J.-P., Coppee, J.-Y., & Colson, A.-M. (1989) *J. Biol. Chem. 264*, 14543–14548.

di Rago, J.-P., Perea, X., & Colson, A.-M. (1986) *FEBS Lett. 208*, 208–210.

Ding, H., Robertson, D. E., Daldal, F., & Dutton, P. L. (1992) *Biochemistry 31*, 3144–3158.

Dutton, P. L. (1978) *Methods Enzymol. 54*, 411–435.

Dutton, P. L. (1986) in *Encyclopedia of Plant Physiology* (Staelin, A., & Arntzen, C. J., Eds.) Vol. 19, pp 197–237, Springer-Verlag, New York.

Dutton, P. L., & Jackson, J. B. (1972) *Eur. J. Biochem. 30*, 495–510.

Glaser, E. G., & Crofts, A. R. (1984) *Biochim. Biophys. Acta 766*, 322–333.

Glaser, E. G., Meinhardt, S. W., & Crofts, A. R. (1984) *FEBS Lett. 178*, 336–342.

Gray, K. A., Davidson, E., & Daldal, F. (1992) *Biochemistry 31*, 11864–11873.

Hacker, B., Barquera, B., Crofts, A. R., & Gennis, R. B. (1993) *Biochemistry 32*, 4403–4410.

Hauska, G., Hurt, E., Gabellini, N., & Lockau, W. (1983) *Biochim. Biophys. Acta 726*, 97–133.

Howell, N., & Gilbert, K. (1988) *J. Mol. Biol. 203*, 607–618.

Howell, N., Appel, J., Cook, J. P., Howell, B., & Hauswirth, W. W. (1987) *J. Biol. Chem. 262*, 2411–2414.

Jackson, J. B., & Crofts, A. R. (1969) *FEBS Lett. 4*, 185–189.

Jackson, J. B., & Dutton, P. L. (1973) *Biochim. Biophys. Acta 325*, 102–113.

Jackson, J. B., Greenrod, J. A., Packham, N. K., & Petty, K. M. (1978) in *Frontiers of Biological Energetics* (Dutton, P. L., Leigh, J. S., & Scarpa, A., Eds.) Vol. 2, pp 316–325, Academic Press, New York.

Knaff, D. B. (1993) *Photosynth. Res. 35*, 117–133.

Kuriyan, J., Wilz, S., Karplus, M., & Petsko, G. A. (1986) *J. Mol. Biol. 192*, 133–154.

McCurley, J. P., Miki, T., Yu, L., & Yu, C.-A. (1990) *Biochim. Biophys. Acta 1020*, 176–186.

Michel, H., Epp, O., & Deisenhofer, J. (1986) *EMBO J. 5*, 2445–2451.

Mitchell, P. (1976) *J. Theor. Biol. 62*, 327–367.

Ohnishi, T., & Trumpower, B. L. (1980) *J. Biol. Chem. 255*, 3278–3284.

Paddock, M. L., Rongey, S. H., Feher, G., & Okamura, M. Y. (1989) *Proc. Natl. Acad. Sci. U.S.A. 86*, 6602–6606.

Paddock, M. L., McPherson, P. H., Feher, G., & Okamura, M. Y. (1990) *Proc. Natl. Acad. Sci. U.S.A. 87*, 6803–6807.

Prince, R. C. (1990) in *The Bacteria: A treatise on structure and function, Vol. XII, Bacterial Energetics* (Krulwich, T. A., Ed.) pp 111–149, Academic Press, Inc., San Diego, CA.

Prince, R. C., Bashford, C. L., Takamiya, K.-I., van der Berg, W. H., & Dutton, P. L. (1978) *J. Biol. Chem. 253*, 4137–4142.

Rao, J. K. M., & Argos, P. (1986) *Biochim. Biophys. Acta 869*, 197–214.

Rich, P. R. (1986) *J. Bioenerg. Biomembr. 18*, 145–155.

Rich, P. R., Jeal, A. E., Madgwick, S. A., & Moody, A. J. (1990) *Biochim. Biophys. Acta 1018*, 29–40.
Robertson, D. E., & Dutton, P. L. (1988) *Biochim. Biophys. Acta 935*, 273–291.
Robertson, D. E., Giangiacomo, K. M., de Vries, S., Moser, C. C., & Dutton, P. L. (1984a) *FEBS Lett. 178*, 343–350.
Robertson, D. E., Prince, R. C., Bowyer, J. R., Matsuura, K., Dutton, P. L., & Ohnishi, T. (1984b) *J. Biol. Chem. 259*, 1758–1763.
Robertson, D. E., Prince, R. C., Davidson, E., van der Berg, W. H., Marrs, B. L., & Dutton, P. L. (1986) *J. Biol Chem. 261*, 584–591.
Robertson, D. E., Daldal, F., & Dutton, P. L. (1990) *Biochemistry 29*, 11249–11260.
Robertson, D. E., Ding, H., Chelminski, P. R., Slaughter, C., Hsu, J., Moomaw, C., Tokito, M., Daldal, F., & Dutton, P. L. (1993) *Biochemistry 32*, 1310–1317.
Salerno, J. C., Xu, Y., Osgood, M. P., Kim, C. H., & King, T. E. (1989) *J. Biol. Chem. 264*, 15398–15403.
Salerno, J. C., Osgood, M., Liu, Y., Taylor, H., & Scholes, C. P. (1990) *Biochemistry 29*, 6987–6993.
Takahashi, E., & Wraight, C. A. (1990) *Biochim. Biophys. Acta 1020*, 107–111.
Takahashi, E., & Wraight, C. A. (1990) *Biochemistry 31*, 855–866.
Trumpower, B. L. (1990) *Microbiol. Rev. 54*, 101–129.
Weber, S., & Wolf, K. (1988) *FEBS Lett. 237*, 31–34.
Weiner, J. H., Cammack, R., Cole, S. T., Condon, C., Honoré, N., Lemire, B. D., & Shaw, G. (1986) *Proc. Natl. Acad. Sci. U.S.A. 83*, 2056–2060.
Westerberg, D. J., Gunsalus, R. P., Ackrell, B. A. C., & Ceccheni, G. (1990) *J. Biol. Chem. 265*, 19560–19567.
Widger, W. R., & Cramer, W. A. (1990) in *The Molecular Biology of Plastids, Vol. 7, Cell Culture and Somatic Genetics of Plants* (Bogorad, L., & Vasil, I. K, Eds.) Academic Press, Inc., San Diego, CA.
Yun, C.-H., Crofts, A. R., & Gennis, R. B. (1991) *Biochemistry 30*, 6747–6754.